plate was subconfluent, cells were treated with 0.25% trypsin/0.5 mM EDTA solution (both from Invitrogen, Tokyo, Japan) and replated at a density of $5 \times 10^3$ cells/ml.

All of the cells were maintained in a humidified incubator at 37° C and 5% $CO_2$. PDLs were calculated using the formula: PDL= log (cell output/input)/log2. At the starting cultivation, PDLs of UCBTERT-21, UCB408E6E7 TERT-33, UE6E7T-3, and UBE6T-6 were 42, 67, 60, and 56, respectively. The doubling time of the UCB408E6E7T-33 cell was 1.5 d, and that of UCBTERT-21, UE6E7T-3, or UBE6T-6 was 2.6, 2.0, or 4.0 days, respectively.

*Measurement of chromosome number and fluorescence in situ hybridization.* Metaphase chromosome spreads for measurement of chromosome number and fluorescence in situ hybridization (FISH) were prepared from exponential growing cells at various PDL. The cells were treated in a hypotonic solution after exposure to 0.06 μg/ml colcemid (Invitrogen, Carlsbad, CA) for 2 h and fixed in methanol/acetic acid (3:1). The cells were spread on a microscope slide.

To count the number of chromosomes, the cells were stained with DAPI (4′-6-diaminido-2-phenylindol; Vector Laboratories, Inc. Burlingame, CA) and examined under an Axioplan II imaging microscope (Carl Zeiss, GmbH) equipped with Leica QFISH software (Leica Microsystems Holding, UK). To examine statistically significant chromosome numbers, we have allowed ±1 deviation and 50–100 metaphase spreads were scored for each assay.

Painting probes specific for chromosome 13 (XCP13-kit, FITC; MetaSystems, GmbH) and chromosome 17 (XCP17-kit; Texas Red) (MetaSystems GmbH, Altlussheim, Germany), and multicolor probes (mFISH-24Xcyte-kit, DAPI, FITC, TexasRed, Cy3, Cy5, and DEAC; MetaSystems GmbH) were used for FISH analysis. FISH was performed according to the manufacture's protocol (MetaSystems GmbH). Briefly, both the metaphase chromosome spread and the probe were denatured with 0.07 N NaOH or 70% formamide, hybridized at 37° C for 1–4 d, and counterstained with DAPI. FISH images were captured and analyzed on the Zeiss Axio Imaging microscope (Carl Zeiss Microimaging GmbH, Jena, Germany) with Isis mBAND/mFISH imaging Software (MetaSystems GmbH).

*CGH analysis.* Hybridization was carried out with the BAC Array (MAC ArrayTM Karyo 4000 Component, Macrogen Co., Rockville, MD) by the Hybstation (Genomic Solutions, Ann Arbor, MI). Briefly, test DNAs, which were isolated using an isolation kit (Amersham BioSciences, Little Chalfont, UK) and Spin Column (QIAGEN Co., Tokyo, Japan), and reference DNAs (Promega Co., Madison, WI), were labeled, respectively, with Cy3 or Cy5 (BioPrimer DNA Labeling System, Invitrogen Co.), precipitated together with ethanol in the presence of Cot-1 DNA, redissolved in a hybridization mixture (50% formamide, 10% dextran sulfate, 2xSSC, 4% sodium dodecyl sulfate [SDS], pH 7), and denatured at 75° C for 10 min. After incubation at 37° C for 30 min, each mixture was applied to an array slide and incubated at 42° C for 48–72 h. After hybridization, the slides were washed in a solution of 50% formamide—2× SSC (pH 7.0) for 15 min at 50° C, in 2× SSC—0.1% SDS for 15 min at 50° C, and in a 100-mM sodium phosphate buffer containing 0.1% Nonidet P-40 (pH 8) for 15 min at room temperature, then scanned with GenePix4000A (Axon Instruments, Union City, CA). Acquired images were analyzed with MacViewer (Macrogen Instruments).

*Differentiation ability.* To evaluate the differentiation potential of each cell line, cells were cultured on a coverslip in each induction medium, that is, hMSC Differentiation BulletKit-Adipogenic (PT-3004, Cambrex BioScience, Inc., Walkersville, MD) for adipocyte and NPMM Bullet kit (NPMM™ BulletKit (B3209, Cambrex BioScience) for neural progenitor cells. For osteoblast, cells were treated with 0.1 μM dexamethasone (Sigma Chemical Co., St. Louis, MO), 50 μg/ml L-ascorbic acid (Sigma Chemical), and 10 mM β-glycerophosphate (Sigma Chemical) in the PLUSOID-M medium (Med-Shirotori Co.) or the POWER-EDBY10 medium (Med-Shirotori Co.) of culture medium.

After 2–4 wk, the cells were washed in phosphate-buffered saline (PBS), fixed in 4% paraformaldehyde in PBS and stained with Oil Red-O (Sigma Chemical) for detection of adipocyte, and with alkaline phosphatase staining solution containing 0.25 mg/ml naphthol AS-BI phosphate and 0.25 mg/ml Fast violet LB salt for detection of alkaline phosphatase-positive osteoblast. In immunostaining for neuron-like cells, the cells fixed with paraformaldehyde were permeabilized with methanol at −20° C for 10 min and stained with an anti-IIIβ tubulin antibody (Sigma Chemical) or anti-neurofilament antibody NF-200 (Sigma Chemical) and Texas Red-anti-mouse IgG (Southern Biotechnology Associates, Inc., Birmingham, AL) as previously described (Takeuchi et al. 1990).

## Results

*Changes in chromosomal number in human mesenchymal stem cell lines in prolonged culture.* Immortalization of cultured cells frequently induces an abnormal chromosome number as shown in cancer cells (Duensing et al. 2000; Munger et al. 2004; Patel et al. 2004), especially at higher frequency in long-term culture. We therefore examined four cell lines, human mesenchymal stem cell (hMSC) lines immortalized with combinations of bmi-1, E6, E7, and/or hTERT genes, for chromosome instability by counting metaphase chromosomes.

All of the lines were diploid, each containing 46 up to 40 PDL including the PDL numbers of nontransfecting original MSCs (Takeda et al. 2004; Mori et al. 2005; Terai et al. 2005). For UCBTERT-21 cell, no further changes in chromosome number have been observed up to date (for PDL 133) as shown in Fig. 1*A* and *B*. In contrast, although the UBE6T-6 cell and the UE6E7T-3 cell were near diploid, both cells exhibited considerable variation in chromosome number from PDL 70 after the culture started. For example, when the assay of UE6E7T-3 cells start at PDL 62 in culture, 90% of cell population had 46 chromosomes, but the population decreased with prolonged culturing and a population containing 44 chromosomes became dominant (43% of cell populations) at PDL 147 (Fig. 1*E*, *F*). A similar variation was also observed in UBE6T-6 cells (Fig. 1*C*, *D*).

To ascertain whether or not the changes observed were induced by transfection with HPV16E6E7, we assayed the chromosome numbers of UCB408E6E7TERT-33 cell in prolonged culture. The cell line showed similar chromosomal changes to those of the UE6E7T-3 cell, the rate of which was more rapid. At day 2 after culture by us changes became evident (PDL 68), the UCB408E6E7TERT-33 cells consisted of two distinct populations concerning chromosome number (near diploid [24%] and near tetraploid [53%]), shown in Fig. 1*G*. However, the near diploid population was unstable and decreased gradually. At PDL 81, the population became only near tetraploid, 80% of the

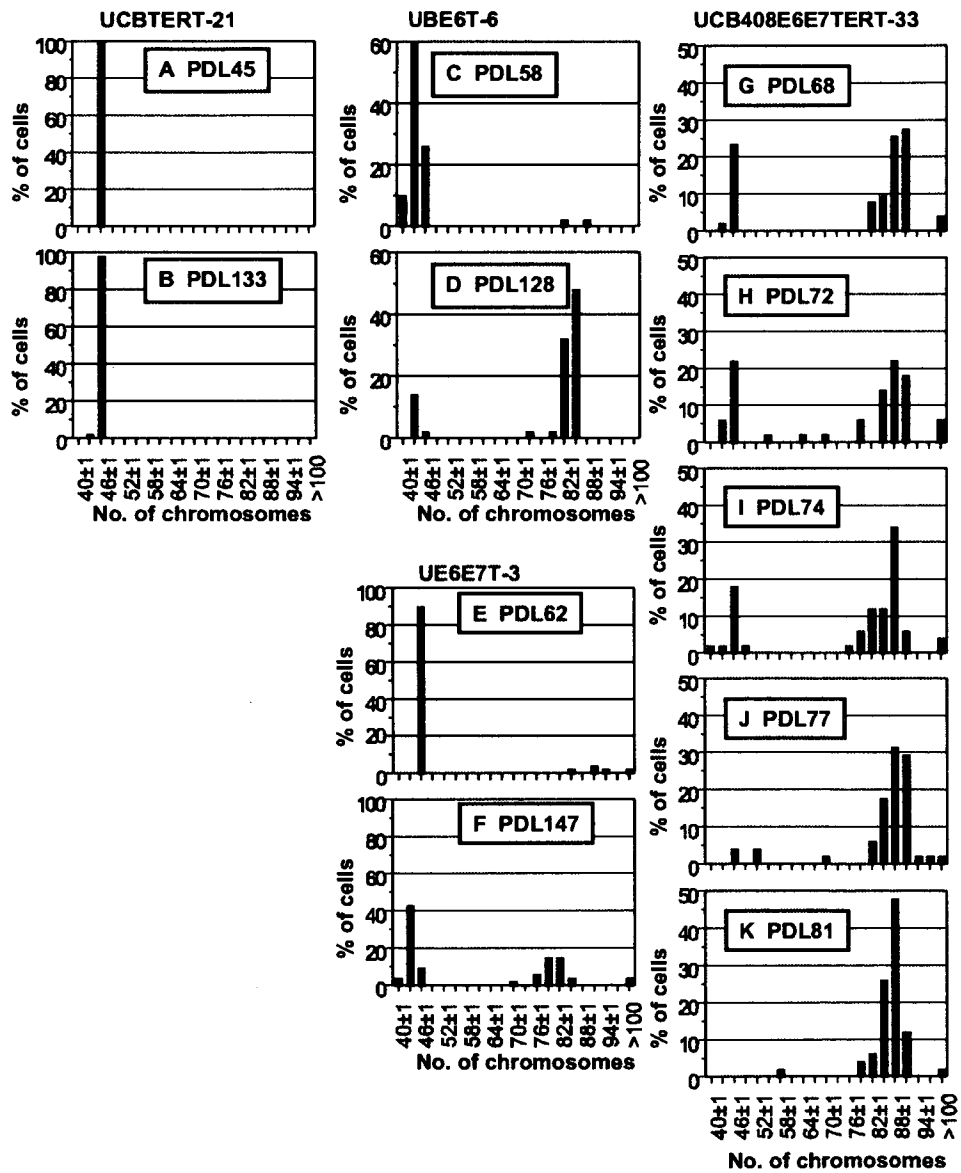


**Figure 1.** Changes in chromosomal numbers in prolonged cultures of four hMSC cell lines. (*A–K*) The chromosomal numbers at various culture stages were counted by DAPI staining. (*A*, *B*), (*C*, *D*), (*E*, *F*), and (*G–K*) represent the chromosomal numbers from UCBTERT-21, UBE6T-6, UE6E7T-3, and UCB408E6E7TERT-33, respectively. To examine statistically significant chromosomal numbers, we have allowed ±1 deviation, and 50–100 metaphase spreads were examined for each assay. *Note* the changes in chromosomal number from near 2*n* to near 4*n* in prolonged culture.

cells contain 85–92 chromosomes (Fig. 1*K*). The results indicate that UCBTERT-21 is relatively stable in chromosome number, whereas each of the oncogene-immortalized cells (UE6E7T-3, UBE6T-6, and UCB408E6E7TERT-33 cell) were unstable in chromosome numbers, which altered substantially during prolonged culture.

We next applied FISH and CGH analysis to characterize the chromosomal aberrations of the cell lines. All of the four cell lines passed for PDL 50 before examination by FISH. mFISH analysis of the UCBTERT-21 cell at PDL 52 showed normal chromosome composition (Fig. 2*A* and *B*) as observed in non-immortalized cells. The UBE6T-6 cell containing 43–45 chromosomes demonstrates losses of chromosome 13, 16, and 19 (marginal variation in chromosome 4 was observed among cells), but keeps on proliferating in chromosome number of 43–45 (Fig. 2*D*, *E*). In contrast, the UCB408E6E7TERT-33 cell showed more heterogeneity in chromosome composition with intrachromosomal and interchromosomal aberrations (data not shown). However, by mFISH analysis we were able to detect nonrandom losses of chromosome 13 in three cell lines except the UCBTERT-21 cell line. This was also confirmed by pFISH analysis using the probes specific for chromosome 13 and chromosome 17 (Fig. 2*C*, *F*). More than 97% of UCBTERT-21 cells showed two copies for chromosome 13, indicating the stability of the chromosomes in the cell line (Fig. 2*G*). The UE6E7T-3 and the UBE6T-6 cell lines with chromosome numbers of 43–45 showed only one copy of chromosome 13 in 76% of UE6E7T-3 cells and 86% of UBE6T-6 cells, respectively (Fig. 2*I*, *J*). A similar loss of chromosome 13 was also observed in 70% of UCB408E6E7TERT-33 cells, which showed three copies of chromosome 13 in near tetraploid (Fig. 2*H*). Other chromosomes, for example chromosome 17, were contained in the UCBTERT-21 and UBE6T-6 cell lines (Fig. 2*C*, *F*).

Furthermore, a significant nonrandom loss of chromosome 13 at the single cell-level observed by FISH was examined by array CGH, which samples the entire cell population. Figure 3 shows the array CGH profiles from early (*blue spots*) and late (*red spots*) stages of proliferating of each cell line. The UCBTERT-21 cell did not show any detectable differences in array CGH profiles between early and late stages (Fig. 3*A*). Although the loss of chromosome 13 had already occurred at early stages in the UBE6T-6 and the UCB408E6E7TERT-33 cell lines, in addition to the losses of chromosomes 4, 9, and 16 (Fig. 3*B*, *D*), in UE6E7T-3 the loss appeared between PDL 78 to 101 with loss of chromosome 16. The most compelling observation was that all three cell lines revealed a consistent whole loss of chromosome 13. These data are consistent with the results observed by FISH analysis. From these results, we

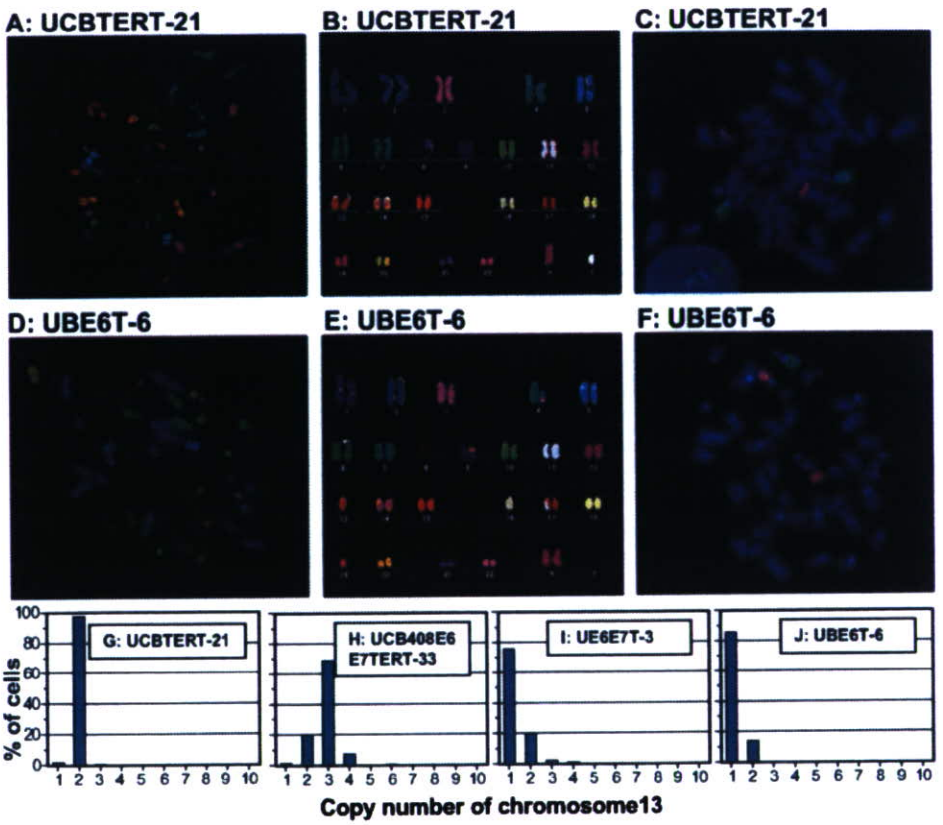


**Figure 2.** FISH analysis of human mesenchymal stem cell (hMSC) lines immortalized with hTERT alone, hTERT plus bm-1, HPVE6 or with hTERT plus HPVE6/E7. Multicolor FISH images of metaphase spreads (*A*, *D*), their karyotypes (*B*, *E*), and painting FISH images using DNA probes specific for chromosome 13 (*green*) and 17 (*red*) (*C*, *F*) of UCBTERT-21 (*A*, *B*, *C*) and UBE6T-6 (*D*, *E*, *F*). Quantity of chromosome 13 copy numbers in four cell lines (*G*–*J*). FISH signals were counted in 120~200 metaphase spreads plus interphase nuclei. UCBTERT-21 cells contained two copies of chromosome 13 and 17, and showed normal human karyotype, whereas other cells lost one copy of chromosome 13.

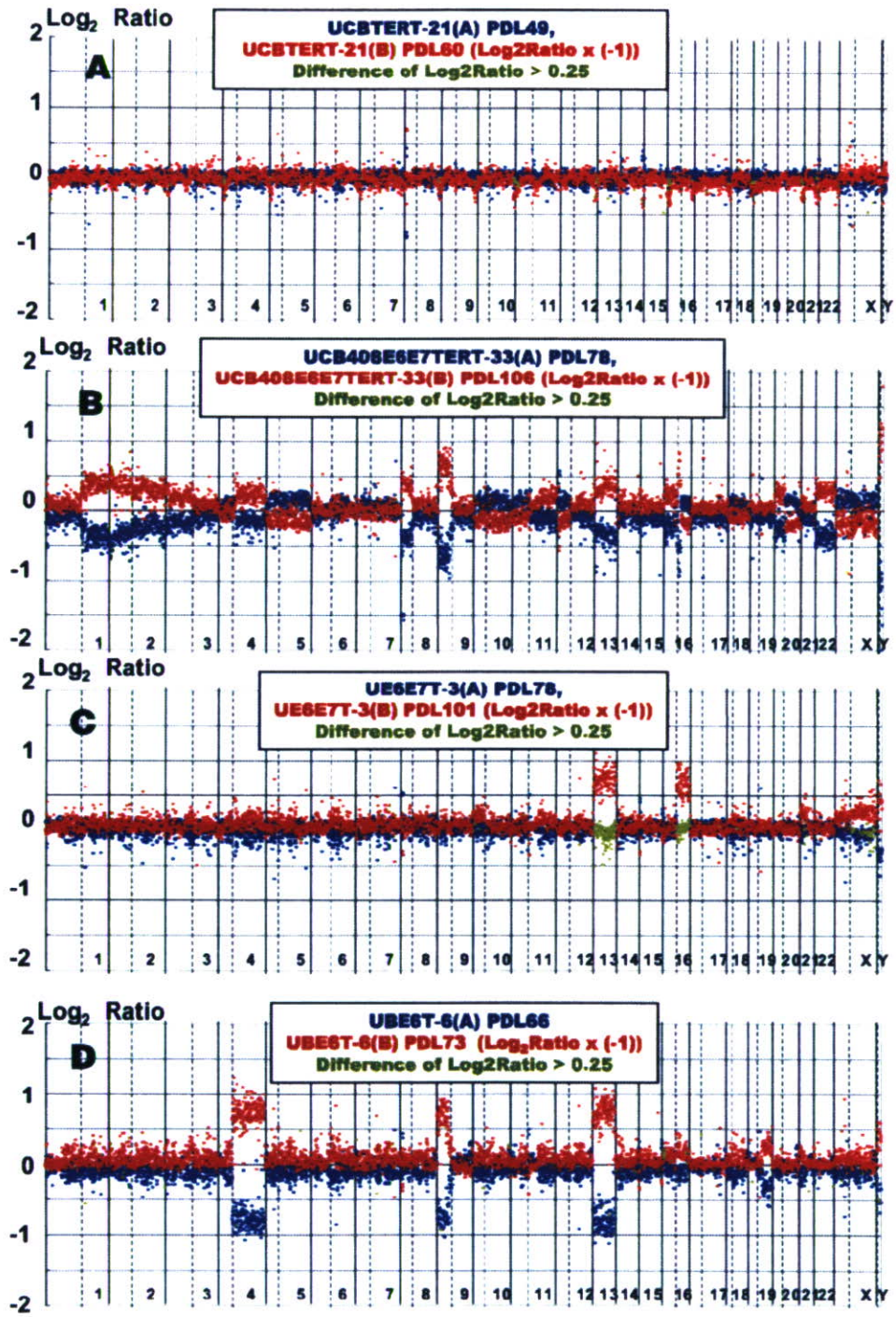


**Figure 3.** Array CGH profiles performed on four immortalized human mesenchymal stem cell lines at selected PDL. For each *panel*, the *X*-axis represents the 22 autosomes, the *X* and *Y* chromosomes, and the *Y*-axis shows the $\log_2$ of the fluorescence intensity ratio (cy3 [hMSCs]/cy5 [normal cell]) of all spots of the chromosome. Values above 0 (*red spots*) or values below 0 (*blue spots*) signify a loss of chromosome (chromosome regions). *Blue spots* in each *panel* indicate the $\log_2$ ratios observed at early stage in the culture of each cell line, which are overlaid with *red spots* indicated at the late stage. *Green spots* indicate the difference in value between *blue spots* and *red spot*. *Note* that in the UE6E7T-3 cell line, one copy of chromosome 13 and 16 were lost between PDL 78 and 101.

concluded that only hTERT-mediated immortalization induced little change in the chromosome numbers and chromosome structures of mesenchymal stem cells, but immortalization with Bmi-1, E6, and E7 in addition to hTERT results in chromosome instability.

*Differentiation potential into lineages of immortalized mesenchymal stem cell lines.* It has been reported that mesenchymal stem cells have the extensive potential to differentiate into multiple cell lineages including osteoblast, chondrocytes, adipocytes (Pittenger et al. 1999), cardiac myocytes (Makino et al. 1999), and neural cells (Pacary et al. 2006; Wislet-Gendebien et al. 2005). To evaluate whether chromosome instability of these cell lines in prolonged culture affects differentiation, cells of each cell line were stimulated in each induction medium for 2 to 4 wk. In

adipocyte-specific culture medium, all cell lines accumulated lipid-rich vacuoles in their cytoplasm within 2 wk, which were made evident by Oil Red-O staining. In particular, the UE6E7T-3 cell line showed a greater adipogenetic ability among the four cell lines (Fig. 4*Ah*). In osteoblast induction medium for 2 wk, UCB408E6E7 TERT-33 cells showed a marked increase in alkaline phosphatase expression, a marker of osteoblast, compared with those in the three other cell lines (Fig. 4*Ad*). In addition, UBE6T-6 cells in neuron induction medium reduced proliferation and displayed marked changes in morphology from being a flat-polygonal shape to taking on the characteristic neuron-like shape in which the cells develop long branching processes. Moreover, in comparing the expression patterns of characteristic neural antigens, i.e., neurofilament, III-β-tubulin, before and after induction (28 d), the pseudo-neural shaped cells showed apparent increases in immunoreactivity to both antibodies (Fig. 4*Af, Ah*),

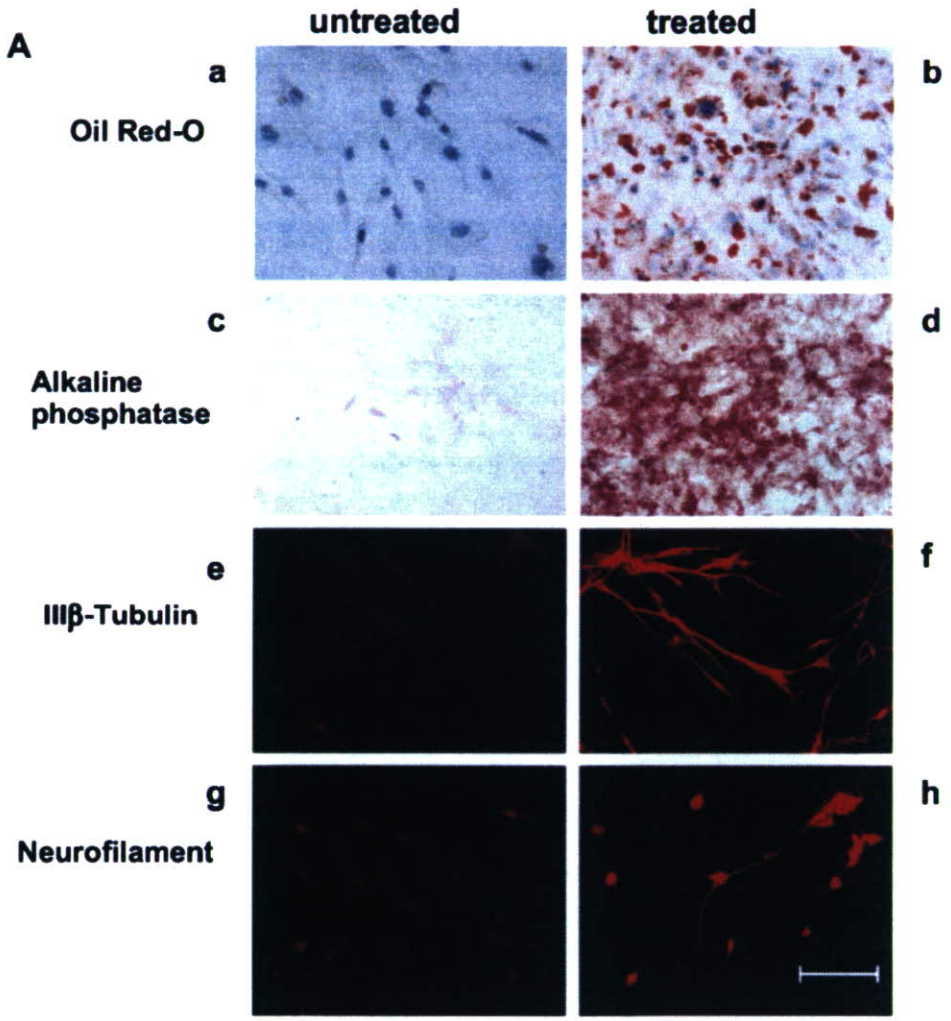


**Figure 4.** Differentiation potential of immortalized human mesenchymal stem cell lines into adipogenic, osteogenic, and neurogenic lineages. Adipogenesis was indicated by the accumulation of lipid stained with Oil Red-O (*Aa* and *Ab*, UE6E7T-3 cell line). Osteogenesis is indicated by the increase in alkaline phosphatase (*Ac* and *Ad*, UCB408E6E7TERT-33 cell line). Neurogenesis was shown by staining with two kinds of monoclonal antibodies to IIIβ-tubulin and neurofilament, and by shape changes of cell (*Ae–Ah*, UBE6T-6 cell line). *B*, Comparison of the differentiation potential of four cell lines whose responses to stimuli into differentiation were diverse among the cell lines. − and + indicate a response similar to an untreated cell and a weak positive response. +++ indicates a strong response shown by images of treated cells in Fig. 4*A*. (*Bar* indicates 20 μm).

B

| | UCBTERT-21 | UCB408E6E7TERT-33 | UE6E7T-3 | UBE6T-6 |
|---|---|---|---|---|
| Oil Red-O | + | ++ | +++ | + |
| Alkarine phosphatase | + | +++ | + | + |
| IIIβ- Tubulin | - | + | +/- | +++ |
| Neurofilament | - | ++ | - | ++ |

whereas such changes were not evident with the flat-shaped cells before induction (Fig. 4*Ae*, *Ag*). Additionally, such cells did not undergo such differentiation in culture medium when cultured for as long as 30 d, although faint staining was observed. Figure 4*B* shows the overall results of differentiation potential of the four cell lines into adipogenic, osteogenic, and neurogenic lineages. These immortalized mesenchymal stem cell lines retained the ability to differentiate into three lineages, although among cell lines there are significant variations in response to lineage-specific induction.

## Discussion

Attempts to clarify the mechanisms for extending the lifespan of tumor cells have been made for many years, and several genes that have effects on cellular proliferation and survival have become clear (Munger et al. 2002) in addition to the elucidation that the majority of tumor cells express telomerase (hTERT; Armanios et al. 2005). The goal of one of the series of our studies has been to establish cell lines with long lifespan and with parental properties, on the basis of genotypic and phenotypic characterizations, for application to cell-based therapy. We previously established several cell lines (Takeda et al. 2004; Mori et al. 2005; Terai et al. 2005), and the present study demonstrated that UCBTERT-21, the immortalized cell line derived from human umbilical cord blood-derived MSCs with hTERT, has a normal karyotype and has an extended lifespan by at least 133 population doublings, and has the differentiation potential into the adipocyte or osteoblast similar to parental MSCs (Terai et al. 2005), although the potential was weak but clearly positive in this study. The specific environmental cues to initiate the differentiation of hMSCs are not yet clear.

UCBTERT-21 immortalized with hTERT alone can be prolonged without inhibition of the $p16^{INK4A}$/RB pathway (Terai et al. 2005), the result of which is in agreement with reports that hTERT alone significantly extends the lifespan of human fibroblasts, epithelial, and endothelial cells (Bodnar et al. 1998; Chang et al. 2005), without the requirement for molecular alterations in p53/p21 and pRB/$p16^{INK4A}$ pathways (Milyavsky et al. 2003). However, other researchers have indicated that inactivation of the RB/p16 pathway by E7, or downregulation of p16 expression, in addition to increasing telomerase activities, is necessary for expanding the lifespan of human keratinocytes (Dickson et al. 2000; Kiyono et al. 1998). Thus, the possibility that a telomere-independent barrier may operate to prevent immortalization according to cell types has been indicated.

UCB408E6E7TERT-33, UE6E7T-3, and UBE6T-6 are hMSC-clones immortalized with HPV16E6/E7 or polycomb group oncogene Bmi-1, in combination with hTERT. Immortalization of human keratinocyte in vitro using virus-derived oncogenes such as E6 and E7 is based on initial inactivation of the p53 and/or Rb pathways, which are essential for controlling cell cycle progression in response to DNA damage or after induction tetraploidy; therefore, this gene transduction induces chromosomal abnormalities (Solinas-Toldo et al. 1997; Duensing et al. 2002; Patel et al. 2004; Schaeffer et al. 2004). The cell lines used in this study became completely immortal, yet underwent dynamic changes in their chromosome numbers in prolonged culture. Near diploid population in early passage of UCB408E6E7 TERT-33 became near-tetraploid population with prolonged culture without the appearance of intermediate populations (60–70 chromosomes/cell), and thereafter gave rise to a population having smaller numbers of chromosomes than tetraploid. Similar patterns existed, although at a slower rate, in UBE6T-6 cells and UE6E7T-3. These results suggest that HPVE6 and E7 proteins cause tetraploidy that precedes the chromosomal aberration to aneuploid in E6/E7-immotalized hMSCs, as is currently shown in several lines of evidence. For example, in vitro experiments in human cell lines (N/TERT-1 keratinocytes and HeLa cells) demonstrate that chromosome nondisjunction yields tetraploid rather than aneuploid, and that aneuploid may develop through chromosomal loss from tetraploid, although the mechanistic basis for the tetraploid formation still remains to be elucidated (Shi et al. 2005). This is also suggested from evidence that high frequency of tetraproidy is present with aneuploidy in human tumors (Olaharski et al. 2006; Sen 2000). A distinct pattern of aneuploid became apparent using dual-probe FISH and CGH analyses, in which UCB408E6E7TERT-33 cells predominantly exhibited triploid 13 and tetraploidy 17 together with other chromosomal changes as shown in Figs. 2 and 3. However, surprisingly, the loss of one copy of chromosome 13 was also seen in 70–80% of diploid UE6E7T-3 and diploid UBE6T-6 cells retaining two copies of chromosome 17. The loss occurred in PDL 50 in both UE6E7T-6 and UCB408E6E7TERT-33, and between PDL 78 and 101 in UE6E7T-3. Structural and numerical aberrations targeting chromosome 17 are often reported in tumors from various tissues (Olaharski et al. 2006), whereas the pattern that chromosome 13 is lost and chromosome 17 is stable, was common for the three cell lines in this study, indicating the possibility that the loss of chromosome 13 may play an important role in the chromosomal aberration of hMSCs to acquire growth advantages under the given culturing condition. Similar karyotypic changes were evident in cultured human embryonic stem cells, involving the gain of chromosome 17 or chromosome 12 (Carlson et al. 2000; Draper et al. 2004). It is thus conjectured that the aneuploidy developed through chromosomal loss from

diploid cells arises through different mechanisms from tetraploid intermediate.

An alternative explanation for aneuploid formation mechanism independent of tetraploid intermediate is loss of regulation in centrosome duplication, leading to abnormal centrosome amplification and multipolar spindles, resulting in aneuploidy. In addition, centrosome amplification caused by loss of p53 has been shown in cultured mouse cells (Fukasawa et al. 1996), but not in cultured human cells (Kawamura et al. 2004). However, loss of p53 and centrosome amplification has been revealed in human cancer tissue. Our preliminary examination has indicated a weak correlation between centrosome amplification and chromosome number (data not shown). Only 2.4% of UCBTERT-21 cells contained >3 centrosomes per cell, whereas 11.9% of UCB408E6E7TERT-33, 19.1% of UE6E7T-3 and 14.3% of UBE6T-6 cells contained >3 centrosomes per cell. Thus, further study is still needed to clarify the mechanism inducing chromosomal instability in immortalized hMSCs cultured over a long period.

Human mesenchymal stem cells are thought to be multipotent cells that can replicate stem cells and that can differentiate to lineages of mesenchymal tissues including bone, fat, tendon, and muscle. Our results indicated that immortalized hMSCs, except UCBTERT-21, induced changes in chromosome number over prolonged culture, but these cells have still retained the ability to both proliferate and differentiate. Immortalized UBE6T-6 cells also displayed neuron-like morphology and strong expression of the neuron-specific markers of neurofilament and III-β-tubulin. We previously demonstrated that hTERT, E7-immortalized hMSCs differentiate into neural cells in vitro on the basis of morphological changes, expression of neural markers such as nestin, neurofilament, MAP-2, Nurr1, and III-β-tubulin. Furthermore, the physiological function showed reversible calcium uptake in response to extracellular potassium concentration (Mori et al. 2005). Similar observations have been reported using rat MSCs (Wislet-Gendebien et al. 2003; Wislet-Gendebien et al. 2005; Pacary et al. 2006). In preliminary experiment of cell transplantation that $10^6$ cells of UCBTERT-21 cell (PDLs 120) or UCB408E6E7TERT-33 cell (PDLs 200) were injected into nude mice subcutaneously, no tumorigenicity was observed (data not shown).

In conclusion, our study showed that the hTERT-immortalized cell line displayed normal karyotype and differentiation ability in prolonged culture. These results provide a step forward toward supplying a sufficient number of cells for new therapeutic approaches. In addition, oncogene-immortalized cell lines exhibited abnormal karyotype accompanying the preferential loss of chromosome 13 but without differential alteration during prolonged culture. Thus, the results could provide a useful model for understanding the mechanisms of the chromosomal instability and the differentiation of hMSC.

**Acknowledgments** This study was supported in part by a grant from the Ministry of Health, Labor and Welfare of Japan. We are grateful to Dr. T.Masui for his advice on ethics problems, and to Mr. H.Migitaka (Carl Zeiss Co., Ltd.) for his assistance with mFISH karyotype analysis. M.T. and K.T. contributed equally to this work.

## References

Armanios, M.; Greider, C. W. Telomerase and cancer stem cells. Cold Spring Harbor Symp. Quant. Biol. 70:205–208; 2005.

Bodnar, A. G.; Ouellette, M.; Frolkis, M.; Holt, S. E.; Chiu, C. P.; Morin, G. B.; Harley, C. B.; Shay, J. W.; Lichtsteiner, S.; Wright, W. E. Extension of life-span by introduction of telomerase into normal human cells. Science 279:349–352; 1998.

Burns, J. S.; Abdallah, B. M.; Guldberg, P.; Rygaard, J.; Schroder, H. D.; Kassem, M. Tumorigenic heterogeneity in cancer stem cells evolved from long-term cultures of telomerase-immortalized human mesenchymal stem cells. Cancer Res. 65:3126–3135; 2005.

Carlson, J. A.; Healy, K.; Tran, T. A.; Malfetano, J.; Wilson, V. L.; Rohwedder, A.; Ross, J. S. Chromosome 17 aneusomy detected by fluorescence in situ hybridization in vulvar squamous cell carcinomas and synchronous vulvar skin. Am. J. Pathol. 157:973–983; 2000.

Chang, M. W.; Grillari, J.; Mayrhofer, C.; Fortschegger, K.; Allmaier, G.; Marzban, G.; Katinger, H.; Voglauer, R. Comparison of early passage, senescent and hTERT immortalized endothelial cells. Exp. Cell Res. 309:121–136; 2005.

Cross, S. M.; Sanchez, C. A.; Morgan, C. A.; Schimke, M. K.; Ramel, S.; Idzerda, R. L.; Raskind, W. H.; Reid, B. J. A p53-dependent mouse spindle checkpoint. Science 267:1353–1356; 1995.

Dickson, M. A.; Hahn, W. C.; Ino, Y.; Ronfard, V.; Wu, J. Y.; Weinberg, R. A.; Louis, D. N.; Li, F. P.; Rheinwald, J. G. Human keratinocytes that express hTERT and also bypass a p16(INK4a)-enforced mechanism that limits life span become immortal yet retain normal growth and differentiation characteristics. Mol. Cell Biol. 20:1436–1447; 2000.

Draper, J. S.; Smith, K.; Gokhale, P.; Moore, H. D.; Maltby, E.; Johnson, J.; Meisner, L.; Zwaka, T. P.; Thomson, J. A.; Andrews, P. W. Recurrent gain of chromosomes 17q and 12 in cultured human embryonic stem cells. Nat. Biotechnol. 22:53–54; 2004.

Duensing, S.; Lee, L. Y.; Duensing, A.; Basile, J.; Piboonniyom, S.; Gonzalez, S.; Crum, C. P.; Munger, K. The human papillomavirus type 16 E6 and E7 oncoproteins cooperate to induce mitotic defects and genomic instability by uncoupling centrosome duplication from the cell division cycle. Proc. Natl. Acad.Sci. U. S. A. 97:10002–10007; 2000.

Duensing, S.; Munger, K. The human papillomavirus type 16 E6 and E7 oncoproteins independently induce numerical and structural chromosome instability. Cancer Res. 62:7075–7082; 2002.

Fukasawa, K.; Choi, T.; Kuriyama, R.; Rulong, S.; Vande Woude, G. F. Abnormal centrosome amplification in the absence of p53. Science 271:1744–1747; 1996.

Harada, H.; Nakagawa, H.; Oyama, K.; Takaoka, M.; Andl, C. D.; Jacobmeier, B.; von, W. A.; Enders, G. H.; Opitz, O. G.; Rustgi, A. K. Telomerase induces immortalization of human esophageal keratinocytes without p16INK4a inactivation. Mol. Cancer Res. 1:729–738; 2003.

Kawamura, K.; Izumi, H.; Ma, Z.; Ikeda, R.; Moriyama, M.; Tanaka, T.; Nojima, T.; Levin, L. S.; Fujikawa-Yamamoto, K.; Suzuki, K.; Fukasawa, K. Induction of centrosome amplification and

chromosome instability in human bladder cancer cells by p53 mutation and cyclin E overexpression. Cancer Res. 64:4800–4809; 2004.

Khan, S. H.; Wahl, G. M. p53 and pRb prevent rereplication in response to microtubule inhibitors by mediating a reversible G1 arrest. Cancer Res. 58:396–401; 1998.

Kiyono, T.; Foster, S. A.; Koop, J. I.; McDougall, J. K.; Galloway, D. A.; Klingelhutz, A. J. Both Rb/p16INK4a inactivation and telomerase activity are required to immortalize human epithelial cells. Nature 396:84–88; 1998.

Makino, S.; Fukuda, K.; Miyoshi, S.; Konishi, F.; Kodama, H.; Pan, J.; Sano, M.; Takahashi, T.; Hori, S.; Abe, H.; Hata, J.; Umezawa, A.; Ogawa, S. Cardiomyocytes can be generated from marrow stromal cells in vitro. J. Clin. Invest. 103:697–705; 1999.

Milyavsky, M.; Shats, I.; Erez, N.; Tang, X.; Senderovich, S.; Meerson, A.; Tabach, Y.; Goldfinger, N.; Ginsberg, D.; Harris, C. C.; Rotter, V. Prolonged culture of telomerase-immortalized human fibroblasts leads to a premalignant phenotype. Cancer Res. 63:7147–7157; 2003.

Mori, T.; Kiyono, T.; Imabayashi, H.; Takeda, Y.; Tsuchiya, K.; Miyoshi, S.; Makino, H.; Matsumoto, K.; Saito, H.; Ogawa, S.; Sakamoto, M.; Hata, J.; Umezawa, A. Combination of hTERT and bmi-1, E6, or E7 induces prolongation of the life span of bone marrow stromal cells from an elderly donor without affecting their neurogenic potential. Mol. Cell Biol. 25:5183–5195; 2005.

Munger, K.; Baldwin, A.; Edwards, K. M.; Hayakawa, H.; Nguyen, C. L.; Owens, M.; Grace, M.; Huh, K. Mechanisms of human papillomavirus-induced oncogenesis. J. Virol. 78:11451–11460; 2004.

Munger, K.; Howley, P. M. Human papillomavirus immortalization and transformation functions. Virus Res. 89:213–228; 2002.

Okamoto, T.; Aoyama, T.; Nakayama, T.; Nakamata, T.; Hosaka, T.; Nishijo, K.; Nakamura, T.; Kiyono, T.; Toguchida, J. Clonal heterogeneity in differentiation potential of immortalized human mesenchymal stem cells3. Biochem. Biophys. Res. Commun. 295:354–361; 2002.

Olaharski, A. J.; Sotelo, R.; Solorza-Luna, G.; Gonsebatt, M. E.; Guzman, P.; Mohar, A.; Eastmond, D. A. Tetraploidy and chromosomal instability are early events during cervical carcinogenesis. Carcinogenesis 27:337–343; 2006.

Pacary, E.; Legros, H.; Valable, S.; Duchatelle, P.; Lecocq, M.; Petit, E.; Nicole, O.; Bernaudin, M. Synergistic effects of CoCl(2) and ROCK inhibition on mesenchymal stem cell differentiation into neuron-like cells. J. Cell Sci. 119:2667–2678; 2006.

Patel, D.; Incassati, A.; Wang, N.; McCance, D. J. Human papillomavirus type 16 E6 and E7 cause polyploidy in human keratinocytes and up-regulation of G2-M-phase proteins. Cancer Res. 64:1299–1306; 2004.

Pittenger, M. F.; Mackay, A. M.; Beck, S. C.; Jaiswal, R. K.; Douglas, R.; Mosca, J. D.; Moorman, M. A.; Simonetti, D. W.; Craig, S.; Marshak, D. R. Multilineage potential of adult human mesenchymal stem cells. Science 284:143–147; 1999.

Saito, M.; Handa, K.; Kiyono, T.; Hattori, S.; Yokoi, T.; Tsubakimoto, T.; Harada, H.; Noguchi, T.; Toyoda, M.; Sato, S.; Teranaka, T. Immortalization of cementoblast progenitor cells with Bmi-1 and TERT. J. Bone Miner. Res. 20:50–57; 2005.

Schaeffer, A. J.; Nguyen, M.; Liem, A.; Lee, D.; Montagna, C.; Lambert, P. F.; Ried, T.; Difilippantonio, M. J. E6 and E7 oncoproteins induce distinct patterns of chromosomal aneuploidy in skin tumors from transgenic mice. Cancer Res. 64:538–546; 2004.

Sen, S. Aneuploidy and cancer. Curr. Opin. Oncol. 12:82–88; 2000.

Shi, Q.; King, R. W. Chromosome nondisjunction yields tetraploid rather than aneuploid cells in human cell lines. Nature 437:1038–1042; 2005.

Solinas-Toldo, S.; Durst, M.; Lichter, P. Specific chromosomal imbalances in human papillomavirus-transfected cells during progression toward immortality. Proc. Natl. Acad. Sci. U. S. A 94:3854–3859; 1997.

Takeda, Y.; Mori, T.; Imabayashi, H.; Kiyono, T.; Gojo, S.; Miyoshi, S.; Hida, N.; Ita, M.; Segawa, K.; Ogawa, S.; Sakamoto, M.; Nakamura, S.; Umezawa, A. Can the life span of human marrow stromal cells be prolonged by bmi-1, E6, E7, and/or telomerase without affecting cardiomyogenic differentiation? J. Gene Med. 6:833–845; 2004.

Takeuchi, K.; Kuroda, K.; Ishigami, M.; Nakamura, T. Actin cytoskeleton of resting bovine platelets. Exp. Cell Res. 186:374–380; 1990.

Terai, M.; Uyama, T.; Sugiki, T.; Li, X. K.; Umezawa, A.; Kiyono, T. Immortalization of human fetal cells: the life span of umbilical cord blood-derived cells can be prolonged without manipulating p16INK4a/RB braking pathway. Mol. Biol. Cell 16:1491–1499; 2005.

Wislet-Gendebien, S.; Hans, G.; Leprince, P.; Rigo, J. M.; Moonen, G.; Rogister, B. Plasticity of cultured mesenchymal stem cells: switch from nestin-positive to excitable neuron-like phenotype. Stem Cells 23:392–402; 2005.

Wislet-Gendebien, S.; Leprince, P.; Moonen, G.; Rogister, B. Regulation of neural markers nestin and GFAP expression by cultivated bone marrow stromal cells. J. Cell Sci. 116:3295–3302; 2003.

Zheng, L.; Lee, W. H. The retinoblastoma gene: a prototypic and multifunctional tumor suppressor. Exp. Cell Res. 264:2–18; 2001.

In Vitro Cell.Dev.Biol. Animal (2007) 43:168–175
DOI 10.1007/s11626-007-9033-5

# Species identification of animal cells by nested PCR targeted to mitochondrial DNA

**Kazumi Ono · Motonobu Satoh · Touho Yoshida · Yutaka Ozawa · Arihiro Kohara · Masao Takeuchi · Hiroshi Mizusawa · Hidekazu Sawada**

Received: 5 March 2007 / Accepted: 17 April 2007 / Published online: 22 May 2007 / Editor: J. Denry Sato


**Abstract** We developed a highly sensitive and convenient method of nested polymerase chain reaction (PCR) targeted to mitochondrial deoxyribonucleic acid (DNA) to identify animal species quickly in cultured cells. Fourteen vertebrate species, including human, cynomolgus monkey, African green monkey, mouse, rat, Syrian hamster, Chinese hamster, guinea pig, rabbit, dog, cat, cow, pig, and chicken, could be distinguished from each other by nested PCR. The first PCR amplifies mitochondrial DNA fragments with a universal primer pair complementary to the conserved regions of 14 species, and the second PCR amplifies the DNA fragments with species-specific primer pairs from the first products. The species-specific primer pairs were designed to easily distinguish 14 species from each other under standard agarose gel electrophoresis. We further developed the multiplex PCR using a mixture of seven species-specific primer pairs for two groups of animals. One was comprised of human, mouse, rat, cat, pig, cow, and rabbit, and the other was comprised of African green monkey, cynomolgus monkey, Syrian hamster, Chinese hamster, guinea pig, dog, and chicken. The sensitivity of the PCR assay was at least 100 pg DNA/reaction, which was sufficient for the detection of each species of DNA. Furthermore, the nested PCR method was able to identify the species in the interspecies mixture of DNA. Thus, the method developed in this study will provide a useful tool for the authentication of animal species.

**Keywords** Cell line authentication · Cross-contamination · Quality control · Bio-resources

K. Ono · M. Satoh (✉) · T. Yoshida · H. Sawada
Health Science Research Resources Bank (HSRRB),
Japan Health Sciences Foundation,
2-11-Rinku-minamihama, Semnan-shi,
Osaka 590-0535, Japan
e-mail: hsrrb@osa.jhsf.or.jp

Y. Ozawa · A. Kohara · M. Takeuchi · H. Mizusawa
Japanese Collection of Research Bioresources (JCRB),
Division of Bioresources,
National Institute of Biomedical Innovation,
7-6-8 Saito-Asagi, Ibaraki-shi,
Osaka 567-0085, Japan

## Introduction

It has been occasionally reported that cell lines derived from a certain source can be contaminated with another cell line. This cross-culture contamination is a serious problem for investigations using culture cells (Nelson-Rees et al. 1981). Therefore, it is very important to confirm the identities of cell lines as part of quality control in the operation of the cell banks that supply these cells to researchers. Some methods have been developed for the authentication of cell lines. For example, short tandem repeat profiling has been used to identify human-origin cell lines (Tanabe et al. 1999; Masters et al. 2001). As for the methods to detect interspecies cross-contamination, chromosome typing, immunological testing, and isoenzyme analysis have been used (Montes de Oca et al. 1969; Stulberg 1973; Doyle et al. 1990). Each of these methods, however, has disadvantages, such as chromosome analysis, which requires great skill, and immunological identification, which requires species-specific antibodies. Isoenzyme analysis is a general method to find

interspecies cross-contamination (Steube et al. 1995). However, the sensitivity of this technique is not suitable for the detection of intermingling with other species-derived cells (Nims et al. 1998), and some specialized reagents and devices are required.

The identification of species by polymerase chain reaction (PCR) based on species-specific deoxyribonucleic acid (DNA) sequences has many advantages, as follows: (1) the equipment required for PCR has become widespread in the laboratories of life science research, (2) the method is relatively simple and does not require great skill, and (3) the sensitivity is high because of amplification of a specific DNA fragment. Thus, some PCR methods for identification of animal species, including cell line authentication, have been reported in recent years (Naito et al. 1992; Hershfield et al. 1994; Parodi et al. 2002; Liu et al. 2003; Steube et al. 2003). However, these methods are not suitable for the purpose of rapidly distinguishing many kinds of animal species.

In the present study, we developed a highly sensitive PCR method that can distinguish 14 animal species, which are commonly used in cell cultures for life science research; i.e., human, cynomolgus monkey, African green monkey, mouse, rat, Syrian hamster, Chinese hamster, guinea pig, rabbit, dog, cat, cow, pig, and chicken.

## Materials and Methods

*Cell lines and preparation of DNA.* All cell lines used in this study are shown in Table 1 and are available from the Health Science Research Resources Bank (HSRRB). These cell lines were confirmed to be free of microorganisms, such as mycoplasma, bacteria, fungi and yeast, and the species in the original description was authenticated by isoenzyme analysis at the HSRRB. Cellular DNA containing both nuclear and mitochondrial DNA was extracted using MagExtractor-Genome (Toyobo. Co., Ltd., Osaka, Japan) according to the manufacturer's instruction, and the resultant purified DNA was used for PCR.

*Primer design.* The information of full-length and partial mitochondrial DNA sequences for 14 species of animals were obtained from the published database at the National Center for Biotechnology Information (NCBI). The accession numbers of the reference sequences and the area corresponding to each primer's target are listed in Table 2, and the nucleotide sequences of each primer are presented in Table 3. The first primers, which were complementary to conserved sequences within cytochrome *b* (for forward primer) and 16S ribosomal RNA genes (for reverse) among the 14 species, were designed as a universal primer pair (Fig. 1). The amplified product covers cytochrome *b*, d-loop, 12S ribosomal RNA and 16S ribosomal RNA genes, and the predicted product size is 4–5 kbp. The species-specific sequences within the area amplified by the universal primer pair were selected as second primer pairs. To clearly identify the species-specific bands in agarose gel electrophoresis, we designed 2nd primers for the 14 species to amplify different sizes of DNA in the range of 200–1400 bp at approximately 50-bp intervals (Table 2; see also Fig. 3*A*).

*Polymerase chain reaction.* The 50-µl reaction mixture contained 1.25 units Takara Ex Taq (Takara Bio, Inc., Otsu, Japan), Ex Taq buffer ($Mg^{2+}$: 2 mM), dNTPs (50 µM each), 10 pmol of each primer and 100 ng of sample DNA, unless otherwise stated. The amplification was carried out in a PCR Thermal Cycler MP (TP3000; Takara Bio Inc.). In the first PCR, the reaction mixture was heated at 94° C for 5 min, at 59° C for 5 min, followed by 35 cycles of elongation at 72° C for 2.5 min, denaturation at 94° C for 30 s, annealing at 59° C for 45 s, with elongation at 72° C

**Table 1.** Cell lines used in this study

| Name of cell line | Registry number | Species |
|---|---|---|
| 293 | JCRB9068 | Human |
| A549 | JCRB0076 | Human |
| COLO320 DM | JCRB0225 | Human |
| HuH-7 | JCRB0403 | Human |
| HeLa S3 | JCRB9010 | Human |
| Hep G2 | JCRB1054 | Human |
| JTC-12 | JCRB0607 | Cynomolgus monkey |
| MK.P3 | JCRB0607.1 | Cynomolgus monkey |
| COS-7 | JCRB9127 | African green monkey |
| Vero | JCRB9013 | African green monkey |
| 3T3-L1 | JCRB9014 | Mouse |
| A9 | JCRB0221 | Mouse |
| B16 melanoma | JCRB0202 | Mouse |
| KUM3 | JCRB1134 | Mouse |
| WEHI-3b | IFO50296 | Mouse |
| C6 | IFO50110 | Rat |
| L6 | JCRB9081 | Rat |
| Py-3Y1-S2 | JCRB0736 | Rat |
| WB-F344 | JCRB0193 | Rat |
| BHK(C-13) | JCRB9020 | Syrian hamster |
| RPMI 1846 | JCRB9087 | Syrian hamster |
| CHO-K1 | IFO50414 | Chinese hamster |
| TG-1 | JCRB0626 | Chinese hamster |
| 104C1 | JCRB9036 | Guinea pig |
| SIRC | IFO50020 | Rabbit |
| MDCK | IFO50071 | Dog |
| CRFK | JCRB9035 | Cat |
| PG4(S+L-) | JCRB9125 | Cat |
| MDBK | JCRB9028 | Cow |
| PK(15) | JCRB9030 | Pig |
| DT40 | JCRB9130 | Chicken |
| LMH | JCRB0237 | Chicken |
| 4G12 hybridoma | IFO50090 | Hybrid (human × mouse) |
| N18-RE-105 | IFO50221 | Hybrid (mouse × rat) |

**Table 2.** The target sequence position for each primer pair in the mitochondrial genome and the predicted size of the amplified product

| Species | Primer | | | | | | Reference mitochondrial DNA sequence (NCBI accession number) |
|---|---|---|---|---|---|---|---|
| | First primer | | Second primer | | | | |
| | Forward | Reverse | Forward | Reverse | Genes amplified | Predicted product size (bp) | |
| Human | 15226–15249 | 2990–3009 | 15311–15334 | 15732–15751 | Cyt b | 441 | NC 001807 |
| Cynomolgus monkey | 479–502[(a)] | 1572–1591[(b)] | 209–229[(c)] | 1320–1340[(c)] | 12S→16S | 1132 | (a)AF295584, (b)AF420036, (c)AF424970 |
| African green monkey | 14643–14666 | 2408–2427 | 800–823 | 1074–1100 | 12S→16S | 301 | AY863426.1 |
| Mouse | 14623–14646 | 2430–2449 | 28–55 | 954–975 | tRNA-Phe→12S | 948 | NC 005089 |
| Rat | 14602–14625 | 2419–2438 | 1748–1767 | 2218–2240 | 16S | 493 | NC 001665 |
| Syrian hamster | 479–502 | ND[a] | 682–703 | 906–926 | Cyt b | 245 | AF119265 |
| Chinese hamster | 14604–14627 | 2413–2432 | 353–376 | 930–953 | 12S | 601 | DQ390542 |
| Guinea pig | 14642–14665 | 2494–2413 | 140–159 | 454–478 | 12S | 339 | NC 000884 |
| Rabbit | 14653–14676 | 2425–2444 | 116–136 | 799–819 | 12S | 704 | NC 001913 |
| Dog | 14668–14691 | 2428–2447 | 1105–1125 | 1838–1859 | 16S | 755 | AY729880 |
| Cat | 15516–15539 | 3288–3307 | 1675–1694 | 3046–3065 | 12S→16S | 1391 | NC 001700 |
| Cow | 14991–15014 | 2781–2800 | 401–421 | 1469–1490 | tRNA-Phe→16S | 1090 | AB074965 |
| Pig | 15791–15814 | 3568–3587 | 2099–2123 | 2898–2917 | 12S→16S | 819 | AY337045 |
| Chicken | 15383–15406 | 3715–3734 | 3395–3415 | 3570–3591 | 16S | 197 | AB086102 |

*Cyt b* cytochrome b, *tRNA-Phe* phenylalanine transfer RNA, *12S* 12S ribosomal RNA, and *16S* 16S ribosomal RNA

[a] The corresponding 16S ribosomal RNA genome sequence of Syrian hamster was not available.

[(a)] means reference sequence AF295584.

[(b)] means reference sequence AF420036.

[(c)] means reference sequence AF424970.

for 10 min in the last cycle, and stored at 4° C. The first amplified product was diluted to 1:10 with sterile distilled water, and a 1 μl aliquot of the diluted product was used as the sample DNA for the second PCR. In the second PCR, the reaction mixture was heated to 94° C for 5 min, maintained at 60° C for 5 min, followed by 30 cycles of elongation at 72° C for 1.5 min, denaturation at 94° C for 45 s, annealing at 60° C for 30 s, with elongation at 72° C for 10 min in the last cycle, and stored at 4° C. Each 5 μl of second PCR product was run on a 2% agarose (SeaKem GTG agarose; Cambrex Bio Science Rockland, Inc., Rockland, ME) minigel unless otherwise noted, stained

**Table 3.** Nucleotide sequences of each primer pair

| Primer pair | Forward sequence | Reverse sequence |
|---|---|---|
| First PCR primer | THGTHSAATGAATCTGAGGVGGVT | CGATGTTGGATCAGGACATC |
| Second PCR primer | | |
| Human | TATTGCAGCCCTAGCAGCACTCCA | AGAATGAGGAGGTCTGCGGC |
| Cynomolgus monkey | AGTGAGCGCAAACGCCACTGC | GTTAACAGTGAAGGTGGCATG |
| African green monkey | CCAGAAGACCCACGATAACTCTCA | TGTTAGCTCAAGGTAATCGAGTTGTAC |
| Mouse | GCACTGAAAATGCTTAGATGGATAATTG | CCTCTCATAAACGGATGTCTAG |
| Rat | CAATCCACCAAGCACAAGTG | CCCCAACCGAAATTTGGTAGTTC |
| Syrian hamster | GACCTCTTAGGTGTATTCCTAC | GTATGAAGAAGGGGTAGAGCA |
| Chinese hamster | CCGGCGTAAAACGTGTTATAGACT | GTATTAGGTATAATATCGGCAGTC |
| Guinea pig | GCCCTATGTACCACACTCAG | CCTTAGCTTTCGTGTGTCGGACTTA |
| Rabbit | CATGCAAGACTCCTCACGCCA | GGGCTTTCGTATATTCTGAAG |
| Dog | GCCCAACTAACCCCAAACTTA | GGTTAACAATGGGGTGGATAAG |
| Cat | TAGAACACCCACGAAGATCC | CATATGGTCTCTTTGGGTCG |
| Cow | CCTAGATGAGTCTCCCAACTC | GTTGTTTAGTCGAGAGGGTATC |
| Pig | CCTATATTCAATTACACAACCATGC | GCGTGTGCGAGGAGAAAGGC |
| Chicken | GTATTCCCGTGCAAAAACGAG | CTTAGTGAAGAGTTGTGGTCTG |

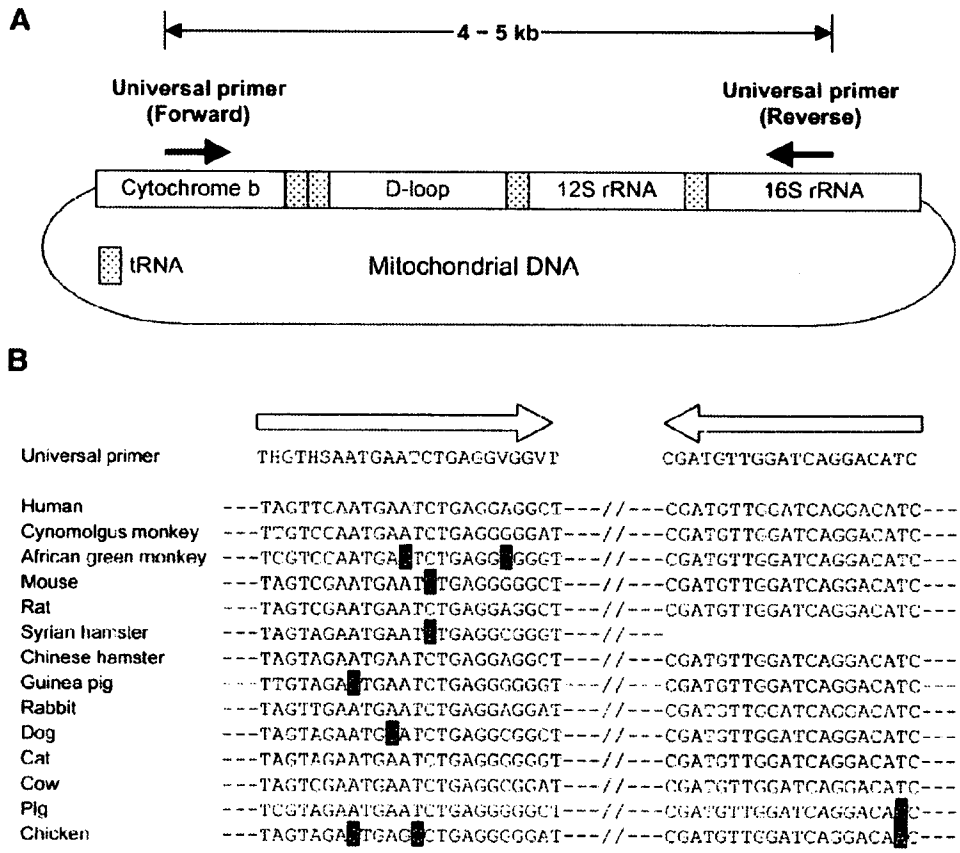


**Figure 1.** Universal primer pairs for the first PCR. (*A*) The target position in the mitochondrial DNA. The first PCR is expected to amplify 4- to 5-kb DNA fragments spanning from cytochrome *b* to 16S rRNA. (*B*) The sequences of the universal primers and the target nucleotide of 14 animal species. The forward primer was designed to be complementary to the conserved sequences within cytochrome *b* and the reverse primer within 16S ribosomal RNA, respectively. Degenerate primer was used for the forward primer, i.e., H:A/C/T, S:C/G, V:A/C/G. Inversed letters indicate bases mismatched to universal primer sequences. The 16S rRNA sequence of Syrian hamster for reverse primer was not available from the NCBI database.

with ethidium bromide, visualized under UV light (MupidScope WD; Advance Co., Ltd., Tokyo, Japan), and photographed. The 100 bp DNA Ladder (Takara Bio Inc.) was applied as a size marker.

## Result and Discussion

*First PCR.* Mitochondrial DNA is generally a desirable target for PCR compared with nuclear DNA, as each animal cell generally contains 500–1,000 copies of mitochondrial DNA. Primers were designed as described in "Materials and Methods". Figure 2 shows the gel electrophoresis of the first PCR products amplified with the universal primer pair from each species DNA. The predicted 4- to 5-kbp products were clearly observed for all species, except for chicken. In the case of chicken, no visible band was observed at ca. 5 kbp, the size predicted from chicken mitochondrial DNA sequence. However, it is likely that specific amplification does occur during the first PCR for chicken DNA, because a much larger amount of chicken DNA was required without first PCR for identification during the second PCR compared with that obtained when first PCR was carried out (data not shown).

*Species-specificity of nested PCR.* The nested PCR strategy was used to specifically amplify species-specific DNA. To confirm amplification by each species-specific primer pair, DNA prepared from each cell line originating from 14 species of animals was subjected to the nested PCR using the universal primer pair in the first PCR and the respective single species-specific primer pair in the second PCR. The amplified product from the corresponding species DNA exhibited the predicted size (Table 2) for each animal species, and could be readily distinguished from each other according to the different sizes (Fig. 3*A*). Figure 3*B* shows the species-specificity of nested PCR in this strategy. Most of the species-specific primer pairs, i.e., human, cynomolgus monkey, Syrian hamster, Chinese ham-

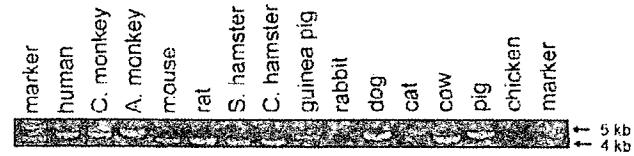


**Figure 2.** Gel electrophoresis of first-PCR products for 14 species. DNA of each species was extracted from the following cell lines indicated in *parentheses*, human (A549), cynomolgus monkey (MK.P3), African green monkey (COS-7), mouse (*WEHI-3b*), rat (Py-3Y1-S2), Syrian hamster (BHK-1 (C-13)), Chinese hamster (CHO-K1), guinea pig (104C1), rabbit (SIRC), dog (MDCK), cat (PG-4(S+L−)), cow (MDBK), pig (PK15), chicken (LMH) for amplification using the universal primer pair. The amplified DNA fragments were run on a 1% agarose gel.

ster, guinea pig, dog, cat, cow, pig, and chicken primers, amplified the specific DNA only from the corresponding species DNA. In the PCR using primer pairs specific for rabbit and African green monkey, however, unexpected bands appeared in addition to the predicted ones. The rabbit primer pair amplified cynomolgus monkey DNA, but the product could be readily distinguished from the rabbit-specific band because of their different sizes. The primer pair for African green monkey also produced an approximately 300-bp-sized band for cynomolgus monkey DNA, which was similar in size

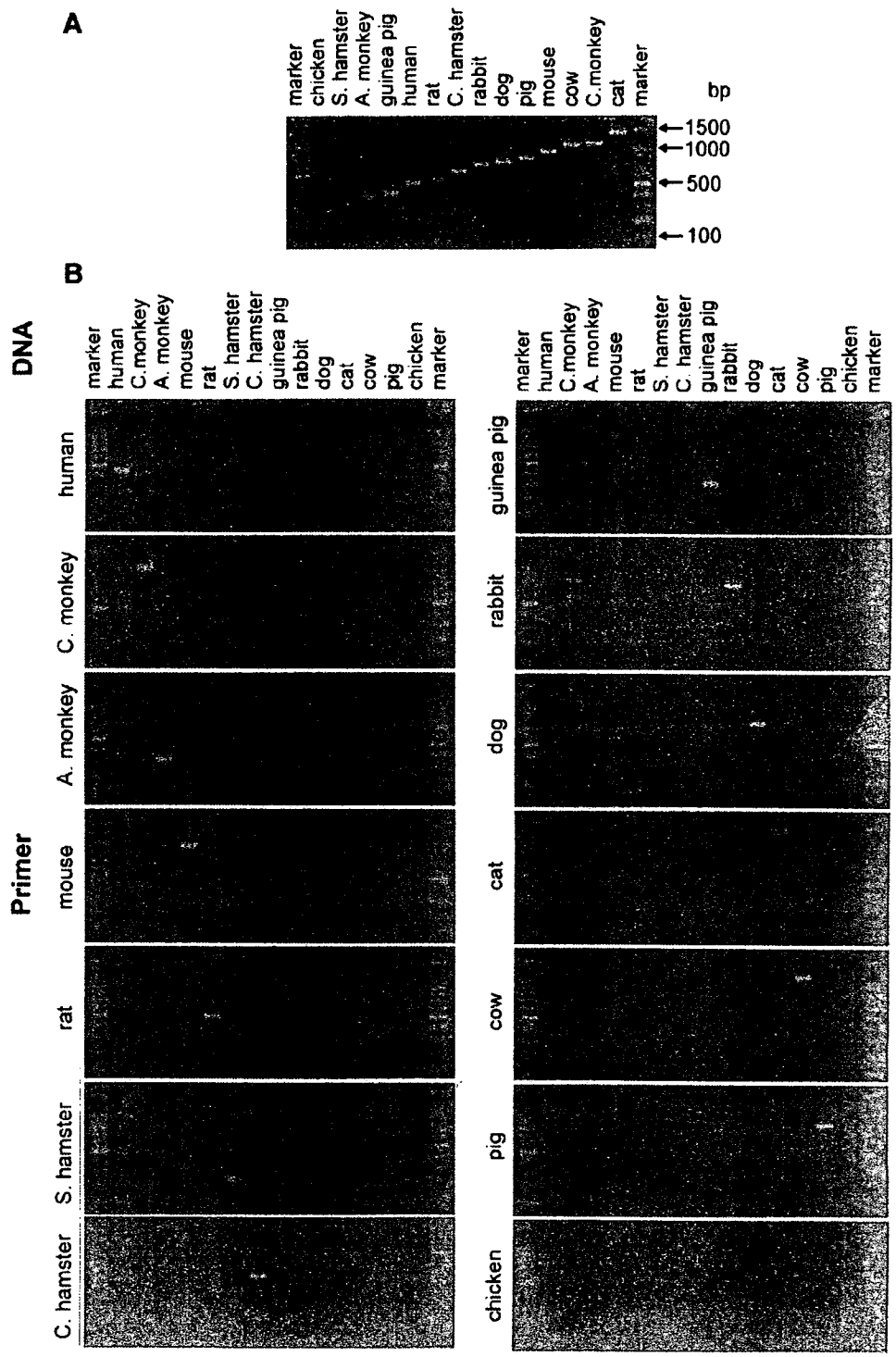


**Figure 3.** Gel electrophoresis of the second-PCR products for 14 species. The same cell lines as in Fig. 2 were used. (*A*) DNA of each species was subjected to nested PCR using corresponding species-specific primer pairs in the second PCR. The second-PCR products were aligned in size-order as a ladder. The amplification products were distinguished by the size. (*B*) Species specificity of the nested PCR. The 14 species-derived DNA was amplified with the universal primer pair and further amplified with the second primer pair indicated on the left side of each photograph.

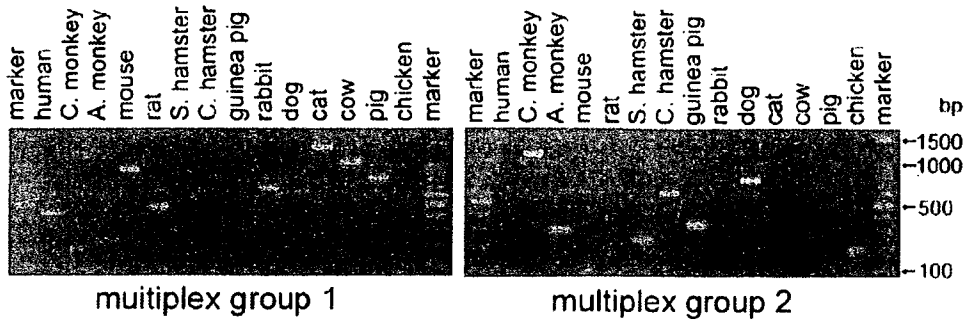


**Figure 4.** Gel electrophoresis of multiplex-PCR products. The first amplification products for 14 species DNA were subjected to multiplex PCR using the mixture of seven species-specific primer pairs as follows. Multiplex group 1: the primer mixture for human, mouse, rat, rabbit, cat, cow, and pig. Multiplex group 2: the primer mixture for cynomolgus monkey, African green monkey, Syrian hamster, Chinese hamster, guinea pig, dog, and chicken. The cell lines used for each animal are the same as described in Fig. 2.

to the African green monkey-specific product. This may be caused by some degree of sequence similarity between African green monkey and cynomolgus monkey in the target mitochondrial DNA. Indeed, when the mixture of primer pairs for African green monkey and cynomolgus monkey were applied to the second PCR, the nonspecific amplified product from cynomolgus monkey DNA disappeared, possibly because of competition of primer annealing to the target DNA sequences (data not shown; *see* also the result in the multiplex PCR section). Thus, it was confirmed that the nested PCR strategy is very useful for the identification of 14 species of DNA.

*Multiplex PCR assay.* For the simple and rapid identification of 14 species of animals, multiplex PCR was examined using primer mixtures in the second PCR. As a result of testing many combinations, it was favorable that the 14 kinds of species-specific primer pairs were divided into two groups as follows: Group 1 contained primer pairs for human, mouse, rat, rabbit, cat, cow, and pig, and Group 2 contained primers for cynomolgus monkey, African green monkey, Syrian hamster, Chinese hamster, guinea pig, dog, and chicken. Figure 4 shows the result of multiplex PCR. These animal species, divided into the two groups, could be clearly detected as species-specific bands. Most of the amplification products were specific for each primer mixture, but nonspecific bands were slightly observed for cynomolgus monkey and African green monkey when multiplex group 1 was used. These nonspecific bands were readily distinguished from the specific ones according to their sizes. Thus, it was found that multiplex PCR assay is applicable to simultaneous identification of 14 species of animals by dividing into two groups. The method developed here is superior to the previous PCR methods (Naito et al. 1992; Hershfield et al. 1994; Parodi et al. 2002; Liu et al. 2003; Steube et al. 2003) in identifying many kinds of species generally used for life science studies. In particular, this method has a great advantage in distinguishing Chinese hamster from Syrian hamster, as the cell lines such as CHO and BHK derived from these two kinds of hamsters are very popular for cell cultures.

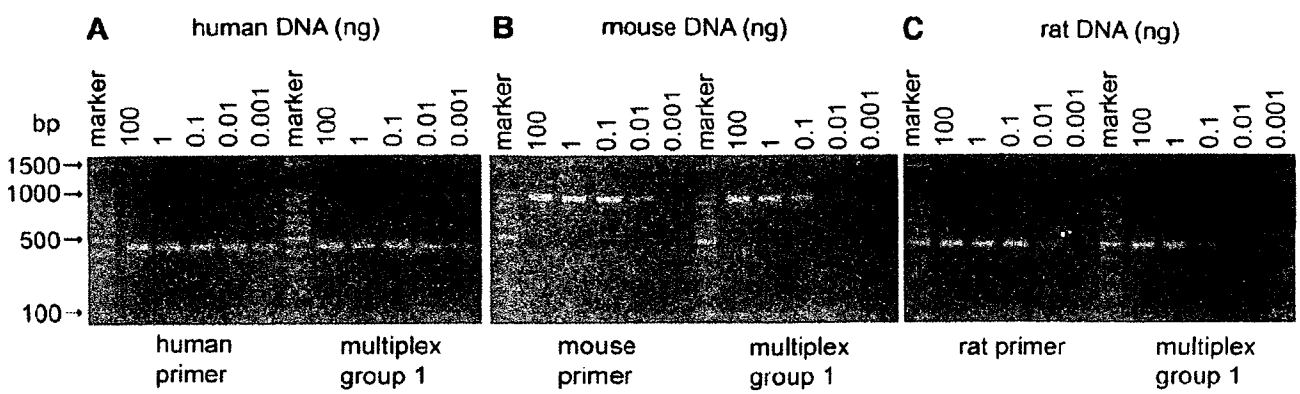


**Figure 5.** Gel electrophoresis of nested-PCR products for serially diluted DNA. The sample DNA was extracted from the human A549 cell line (*A*), mouse WEHI-3b cell line (*B*), and rat Py-3Y1-S2 cell line (*C*), and diluted serially to the nested PCR. The product bands amplified by single species-specific primer pairs are shown on the *left side* and those by multiplex group 1 are on the *right* in each photograph.

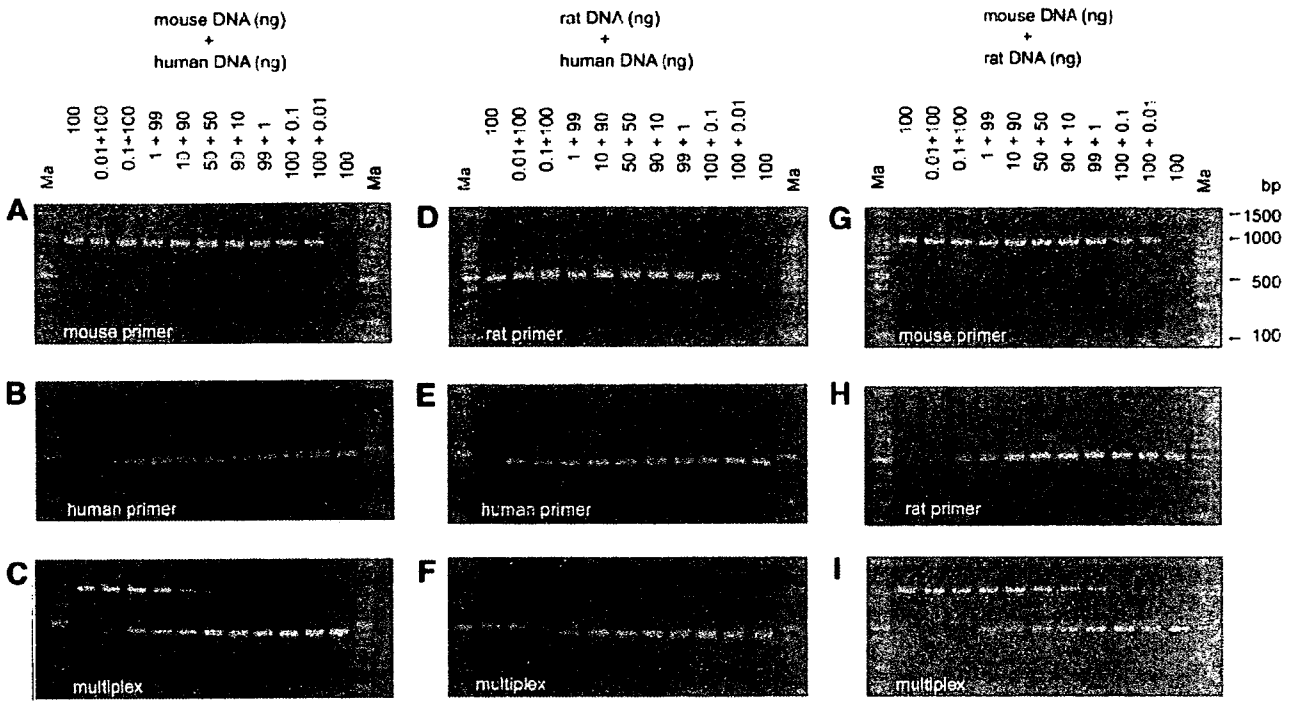


**Figure 6.** Gel electrophoresis of nested-PCR products for interspecies DNA mixtures. Two kinds of DNA, such as human and mouse DNA (*A*, *B*, *C*), human and rat DNA (*D*, *E*, *F*), and mouse and rat DNA (*G*, *H*, *I*) were mixed in various ratios for amplification with nested PCR. The cell lines used were the same as in Fig. 5. In the second PCR, the single species-specific primer pairs (*A*, *B*, *D*, *E*, *G*, *H*) or the multiplex group 1 (*C*, *F*, *I*) were used.

*Sensitivity of PCR assay.* Serially diluted cellular DNA was amplified with the nested PCR using either the corresponding species-specific primer pair or the mixture of seven species-specific primer pairs (multiplex PCR described above) as the second PCR primer. Each of the 14 species of DNA was detectable from at least 100 pg DNA/reaction by both PCR assays. Figure 5 shows the sensitivity of the PCR assay, as an example, using DNA prepared from human, mouse, and rat cell lines, which are commonly used for cell culture experiments. The amount of DNA required for identification of each species was 10 pg/reaction or more for the single species-specific primer pair as the second primer, and 100 pg/reaction or more for the multiplex assay. The sensitivity of the multiplex assay was somewhat low compared to the species-specific single primer.

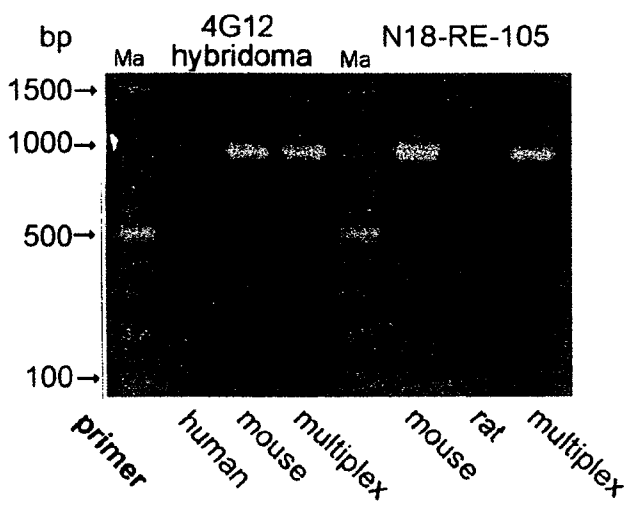


**Figure 7.** Gel electrophoresis of nested-PCR products for DNA derived from interspecies hybrid cell lines. DNA from 4G12 hybridoma (human × mouse) and N18-RE-105 (mouse × rat) were applied to nested PCR. Multiplex group 1 or the corresponding species-specific primer pairs were used in the second PCR.

*Identification of species from interspecies DNA mixtures.* The possibility of cross-contamination or replacement of cells exists during the process of cell preparation. As part of the quality control of cell lines in the cell bank, it is very important to verify the source species of each derived cell line. For that purpose, we attempted to identify the species from interspecies DNA mixtures. Two species of DNA, among human, mouse and rat, were mixed in various ratios for the nested PCR. When the single species-specific primer pair was used in the second PCR, each species of DNA was sensitively detected even when two kinds of DNA were present in the mixture. For example, when mouse-specific primers were used, a mouse-specific band was detected in the DNA mixture composed of 100 ng human or rat DNA + 10 pg mouse DNA (Fig. 6*A*, *G*). Likewise, in the case of human-specific or rat-specific primers alone, their respective species-specific band was also detected at 10 pg DNA

(Fig. 6*B, E, D, H*). When group 1 of the multiplex primers (seven species-specific primer pairs composed of human, mouse, rat, rabbit, cat, cow, and pig) was used at the standard concentration (10 pmol each species-specific primer/50-μl reaction), the sensitivity apparently decreased and there was considerable difference in the sensitivity for human, mouse, and rat DNA (Fig. 6*C, F, I*). This may be caused by the different amplification efficiency of each species-specific primer in the simultaneous reaction. Indeed, by decreasing the ratio of human primer pairs relative to the others, the sensitivity for mouse and rat DNA clearly increased (data not shown). Thus, this method will likely become a very useful tool for quickly detecting cross-contamination, and the sensitivity in the multiplex assay will be further increased by optimizing the concentration and the ratio of species-specific primers.

*Hybrid cell lines.* We applied this PCR method to original-species verification of interspecies hybrid cell lines. The hybrid cell lines of 4G12 (human B lymphocytes × mouse myeloma cell line; Saito et al. 1988) and N18-RE-105 (mouse glioma cell line × rat neural retina cells; Malouf et al. 1984) were tested by isoenzyme analysis and nested PCR. Although the original species were confirmed by isoenzyme analysis of both hybridomas between human and mouse, and between mouse and rat, only the mouse-specific band was observed for both hybridomas by nested PCR (Fig. 7). This result is consistent with the previous reports that the mouse mitochondria dominate selectively in these hybrid cells, whereas human or rat mitochondria are ultimately excluded from the hybrid cells (Attardi and Attardi 1972; Yamaoka et al. 2001). The nested PCR method targeted to the mitochondria genome was not applicable to the parental species identification of interspecies hybrid cells.

## References


Attardi, B., Attardi, G. Fate of mitochondrial DNA in human-mouse somatic cell hybrids. Proc Nat Acad Sci USA. 129–133; 1972.

Doyle, A., Morris, C., Mowles, J. M. Quality control. In: Doyle, A, Hay, R., Kirsop, B. E. eds. Living resources for biotechnology. Animal cells. Chapter 5. Cambridge: Cambridge University Press; 1990: 81–100.

Hershfield, B., Chader, G., Aguirre, G. A polymerase chain reaction-based method for the identification of DNA samples from common vertebrate species. Electrophoresis. 15: 880–884; 1994.

Liu, M. Y., Lin, S., Liu H., Candal, F., Vafai A. Identification and authentication of animal cell culture by polymerase chain reaction amplification and DNA sequencing. In Vitro Cell Dev Biol Anim. 39: 424–427; 2003.

Malouf, A. T., Schnaar, R. L., Coyle, J. T. Characterization of a glutamic acid neurotransmitter binding site on neuroblastoma hybrid cells. J Biol Chem. 259: 12756–12762; 1984.

Masters, J. R., Thomson, J. A., Daly-Burns, B., Reid, Y. A., Dirks, W. G., Packer, P., Toji, L. H., Ohno, T., Tanabe, H., Arlett, C. F., Kelland, L. R., Harrison, M., Virmani, A., Ward, T. H., Ayres, K. L., Debenham, P. G. Short tandem repeat profiling provides an international reference standard for human cell lines. Proc Nat Acad Sci USA. 98: 8012–8017; 2001.

Montes de Oca, F., Macy, M. L., Shannon, J. E. Isoenzyme characterization of animal cell culture. Proc Soc Exp Biol Med. 132: 462–469; 1969.

Naito, E., Dewa, K., Yamanouchi, H., Kominami, R. Ribosomal ribonucleic acid (rRNA) gene typing for species identification. J Forensic Sci. 37: 396–403; 1992.

Nelson-Rees, W. A., Daniels, D. W., Flandermeyer, R. R. Cross-contamination of cells in culture. Science. 212: 446–452; 1981.

Nims, R. W. Shoemaker, A. P., Bauernschub, M. A., Rec L. J., Harbell, J. W. Sensitivity of isoenzyme analysis for the detection of interspecies cell line cross-contamination. In Vitro Cell Dev Biol Anim. 34: 35–39; 1998.

Parodi, B., Aresu, O., Bini, D., Lorenzini, R., Schena, F., Visconti, P., Cesaro, M., Ferrera, D., Andreotti, V., Ruzzon, T. Species identification and confirmation of human and animal cell lines: a PCR-based method. BioTechniques. 32: 432–440; 2002.

Saito, H., Uchiyama, K., Nakamura, I., Hiraoka, H., Yamaguchi, Y., Taniguchi, M. Characterization of a human monoclonal antibody with broad reactivity to malignant tumor cells. J Natl Cancer Inst. 80. 728–734; 1988.

Steube, K. G., Grunicke, D., Drexler, H. G. Isoenzyme analysis as a rapid method for the examination of the species identity of cell cultures. In Vitro Cell Dev Biol Anim. 31: 115–119; 1995.

Steube, K. G., Meyer, C., Uphoff, C. C., Drexler, H. G. A simple method using β-globin polymerase chain reaction for the species identification of animal cell lines—a progress report. In Vitro Cell Dev Biol Anim. 39: 468–475; 2003.

Stulberg, C. S. Extrinsic cell contamination of tissue culture. In: Fogh, J. ed. Contamination in tissue culture. New York: Academic Press; 1973:2–23.

Tanabe, H., Takada, Y., Miregishi, D., Kurematsu, M., Masui, T., Mizusawa, H. Cell line individualization by STR multiplex system in the cell bank found cross-contamination between ECV304 and EJ-1/T24. Tissue Culture Research Communications. 18: 329–338; 1999.

Yamaoka, M., Mikami, T., Ono, T., Nakada, K., Hayashi, J. Mice with only rat mtDNA are required as models of mitochondrial diseases. Biochem Biophys Res Commun. 282: 707 711; 2001.

Tiss. Cult. Res. Commun. 26: 159–163 (2007)


# 培養細胞研究資源のマイコプラズマ汚染調査

小原　有弘[1,2]、大谷　梓[1]、小澤　裕[1]、塩田　節子[1]、増井　徹[1]、水澤　博[1,2]

[1] 独立行政法人医薬基盤研究所生物資源研究部細胞資源研究室　〒567-0085　大阪府茨木市彩都あさぎ7-6-8
[2] 日本組織培養学会、細胞バンク委員会

【要約】　マイコプラズマは自己増殖能を持つ、細菌の1/10程度の大きさの微生物で培養細胞と共存して増殖する汚染しやすい微生物とされているが、培地が濁ることがないので混入に気付きにくい。しかし、マイコプラズマ汚染が研究に及ぼす影響は多大であり、サイトカインの発現異常、染色体の異常、細胞死などを引き起こし、その混入を軽視することはできない。そこで日本組織培養学会細胞バンク委員会と JCRB 細胞バンクは協力して、マイコプラズマ簡易迅速検査キット「MycoAlert®」を利用したマイコプラズマ汚染に関する全国実態調査を開始し、今までに11大学、２国立研究所、３企業の協力が得られている。既に1500検体程度の解析を実施したが、平均汚染率は22.4%という結果を得たのでその概略を中間報告として紹介する。今後我々は、さらに調査を進めると共に、細胞に汚染していたマイコプラズマ種の同定も行い汚染源の特定なども行いながら、マイコプラズマ汚染の予防法や除去法についての紹介も今後行っていきたいと考えている。

【キーワード】　マイコプラズマ、マイコプラズマ汚染、MycoAlert®

## マイコプラズマについて

マイコプラズマは *Mollicutes*（モリキューテス）綱に属する微生物であり、自己増殖能を持つ最小のバクテリアとされている。ゲノムサイズは55万塩基対程度と細菌の1/10ほどの大きさで（300 nm–1000 nm）、0.22 μm のフィルターを通過する。細胞壁は持たないためにペニシリン系抗生物質は無効で、カナマイシンやゲンタマイシンなどに耐性を持つものが多いなどの特徴をもっている。マイコプラズマには非常に多くの種類が存在することがわかっているが、細胞を汚染するマイコプラズマの種類は限られており、*M. Arginini*（自然宿主：ヒト・ヤギ、生息部位：口腔咽頭・尿生殖器）、*M fermentans*（自然宿主：ヒト、生息部位：尿生殖器）、*M hyorhinis*（自然宿主：ブタ、生息部位：鼻腔）、*M. orale*（自然宿主：ヒト、生息部位：口腔咽頭）、*A. laidlawii*（自然宿主：ウシ、生息部位：口腔咽頭・尿生殖器）、*M. salivarium*（自然宿主：ヒト、生息部位：口腔咽頭）の６種類が全汚染の96%を占めていると言われている。現在では細胞

連絡者：小原有弘
独立行政法人医薬基盤研究所生物資源研究部細胞資源研究室
〒567-0085　大阪府茨木市彩都あさぎ7-6-8
TEL：072-641-9851、FAX：072-641-9851
E-mail: kohara@nibio.go.jp

培養に用いる血清や添加物などの製品の品質が改良されてきたことに伴い、マイコプラズマの汚染源となるところは変わってきたと思われるが、研究に利用されている培養細胞のマイコプラズマ汚染は未だに減少していないとも言われている。そこで、我々は実態把握のための広範囲な国内調査が必要であると考えた。

## 細胞のマイコプラズマ汚染検出法

マイコプラズマの検出法の主なものには分離培養法、DNA 蛍光染色法、ネスティッド PCR 法があり日本薬局方や JIS 規格によって定められてきた。分離培養法はその名の通り、マイコプラズマを培養してその有無を確認する方法でありコロニーが生成すれば正確な結果を期待できるが、検査には嫌気培養法なども使わなければならないなどの面倒な点も多いうえに検査に要する期間も 2 週間から 3 週間程度かかってしまう。また、まだ分離用培地が開発されていないマイコプラズマ種も確認されていることなどから我々が日常的な検査に用いるには適切な方法とはいえない。そこで、細胞バンクでは DNA 蛍光染色法とネスティッド PCR 法の二つの方法を細胞の品質検査に採用して実施してきた。この 2 つの検出方法はともに高感度で確実な結果が出る点と、検査に要する時間が分離培養法に比べて短期間ですむ点が有利であった。それでも検査を始めてから結果が出るまでには 1 週間以上もの時間を要してしまう点が、マイコプラズマ汚染検査が一般にはなかなか普及しないという理由となっているように思われた。そのような中で最近になって MycoAlert® (Lonza Rockland, Inc. ME, USA) 法という、およそ20分程度でマイコプラズマ混入に関する検査結果が得られるという、迅速な試験キットが市販されることとなった。そこで、JCRB 細胞バンクでは2007年 5 月に開催

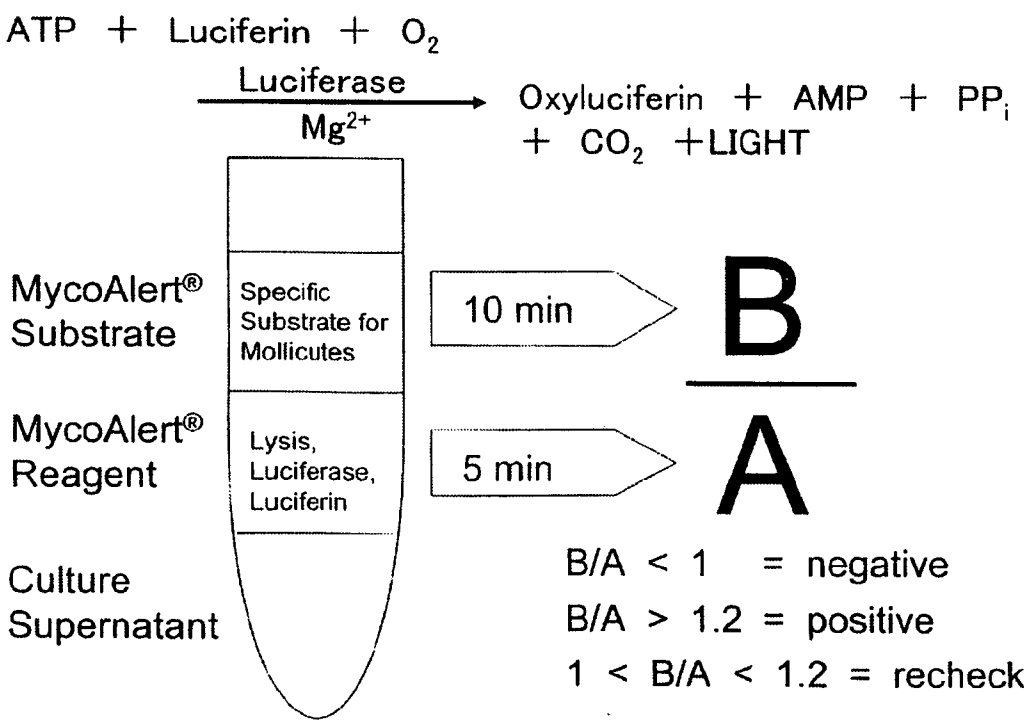


図 1　測定の原理と結果の判定
測定に用いるのは培養上清100 μLで、MycoAlert® Reagent を添加して 5 分後にルミノメータによりバックグラウンド値を測定し、MycoAlert® Substrateを添加して10分後にマイコプラズマ特有の酵素活性を測定する。

された日本組織培養学会（第80回大会）を契機に、日本組織培養学会の細胞バンク委員会と協力をして、我国のマイコプラズマ汚染に関する全国実態調査を試みることにした。MycoAlert®法の特徴を生かせば多数の試料を短時間で処理することができるので、我国におけるマイコプラズマ汚染の実態調査が可能になるのではないかと考えたのである。また、こうした調査を通じて検査が容易であることに気づいて頂ければ、マイコプラズマ汚染検査を日常的に実施する習慣を身に付けることが可能になるのではないかとも考えたところである。

MycoAlert®法はルミノメーターを用いてマイコプラズマに特異的な酵素反応を検出するものである。細胞の培養上清 100 μL を用い、小数の試薬を添加してからルミノメーターで光度を測定するだけなので20分ほどで結果が出る。そのため、忙しい実験の合間にマイコプラズマ汚染の有無をチェックしてしまうことも可能であろう。検査の概略は図 1 に示した。細胞の培養上清（100 μL）に MycoAlert® Reagent（試薬）を添加して 5 分後に反応液中の ATP とルシフェラーゼによるバックグラウンド値をルミノメーターで測定し、その後 MycoAlert® Substrate（基質）を添加して10分後に再度ルミノメーターで値を読み取る。培養上澄にマイコプラズマが存在していればこの 2 回目の読み取り値が上昇する。この上昇がマイコプラズマに特異的な酵素の反応によるものである。この値を最初に測定したバックグランド値で割った値を用いてマイコプラズマの有無を判定した。この比が 1.2 以上なら陽性、1.0 未満は陰性、1.0 以上 1.2 未満を要再検査と判定した。

## マイコプラズマ汚染検査結果

これまでに11の大学、2 つの国立研究所、3 社の企業と JCRB 細胞バンクが所属する（独）医薬基盤研究所に依頼して収集した1470検体について三光純薬（株）（販売元）の協力を得て検査を実施し、陽性330検体、陽性率22.4％という結果（表 1）を得た。調査では大学の研究室からのサンプルが多く汚染率も平均値を上回った。また、国立研究所や企業は比較的低いという結果であったがサンプル数が少ないので今後さらに調査を進めて確認したい。個別の研究室の汚染率については、それらのデータを示すことは出来ないが、研究室ごとにばらついており、今回の平均値より高い値が出た研究室では十分に注意をされたい。大学で比較的高い汚染率が出たことについては色々な理由が考えられると思われるが、学生の入れ代わりが多い点にも原因があるのではないだろうか。十分な教育が必要であることを物語っているように感じられる。

表 1　マイコプラズマ汚染検査結果

| 検体提供機関 | 検体数 | 陽性検体数 | 汚染率 |
|---|---|---|---|
| 大学（11大学） | 1116 | 284 | 25.4% |
| 国立研究所（2 機関） | 58 | 1 | 1.7% |
| 企業（3 社） | 46 | 5 | 10.6% |
| 医薬基盤研究所 | 250 | 40 | 16.0% |
| 合計 | 1470 | 330 | 22.4% |

国立研究所、企業におけるマイコプラズマ汚染率は大学におけるマイコプラズマ汚染率よりも低い。

なお、我々は、ここで得られた結果を確認するために、これらのサンプルをランダムに選択してさらにネスティッド PCR 法や蛍光染色法を実施してマイコプラズマの有無を確認した。その結果はここで示した MycoAlert®法の結果と矛盾することは無かった（データは示さない）。

## マイコプラズマ除去法

マイコプラズマは先にも述べたようにヒトに常在する微生物であり、樹立当初は汚染されていなかった細胞も研究の過程で汚染してしまう可能性

が十分にあるので注意しなければならない。汚染除去には抗生物質を用いて汚染細胞を処理することになるが、マイコプラズマにも薬剤耐性が出現していることが知られており、抗生物質が効かないマイコプラズマ種も存在しているようである。また、マイコプラズマを除去する薬剤が細胞に与える影響も十分に考えなければならず、その影響により細胞の性質が変わることもあるので、抗生物質処理を行った場合は除去後細胞の性質を再確認する必要もある。除去に用いられる抗生物質は、キノロン系の MC-210（大日本住友製薬製）やプレウロムチリンとテトラサイクリンの誘導体2つの抗生物質より構成される BM-サイクリン（ロシュ社製）が利用されることが多いが、マイコプラズマ汚染の除去には色々な方法を組み合わせてやっと除去に成功するなど悪戦苦闘することも多く手間がかかる作業である。JCRB 細胞バンクではこれまでに50株程度の培養細胞についてマイコプラズマ汚染除去を試みて9割程度で成功した実績を有している。ただ、MC210 などの新しい試薬がマイコプラズマの除去に有効であるからといって、これらの試薬をけして日常的に培養液に添加して培養するなどの方法を取ってはならない。こうした安易な取り扱いは MC210 耐性菌を増やし、マイコプラズマ除去を不可能にしてしまうので注意すべきである。

こうした薬剤によるマイコプラズマ除去を試みる場合は、薬剤の仕様書に従って注意深く行うべきである。

## マイコプラズマ汚染の予防

今回の調査では培養細胞のマイコプラズマ汚染率の平均値は22.4%であった。この数字は30年前とほぼ同じであり、血清や培地添加物の品質が向上してマイコプラズマの汚染源とならなくなったにもかかわらず未だに高い汚染率で推移していると言わざるを得ない。マイコプラズマに汚染されてしまったら除去を考えざるを得なくなるが、汚染しないように予防するほうが遥かに有意義であるし、研究へのコストも低く抑えられる。

マイコプラズマはヒトの口の中にも常在する微生物なので、培養作業中に唾液が飛べば汚染の原因となる。従って、十分に整備された実験環境（クリーンベンチ、安全キャビネット使用）でゴム手袋やマスクの着用を心がけたとしても、実験中に話をすれば、それが汚染の原因になってしまう。そのため、それぞれの実験実施者が汚染の拡大を防ぐ意識を持って、私語を慎むなど自制することが重要だと思われる。また、マイコプラズマの汚染の拡大は汚染された細胞から非汚染細胞へ移ることも多いと言われている。特に、培地を介しての汚染の拡大はクロスコンタミネーションの原因ともなると考えられているので、ピペット等を培養中の細胞と培地瓶の間を往復させずに一方向になるような操作を心がける必用があろう。さらに、マイコプラズマで汚染した培地を実験台にこぼしてしまったような場合にも、いずれ乾いてしまうから大丈夫だろうとはけして考えず、すぐに殺菌剤を含む布巾でぬぐい取っておくなどの配慮が必要である。培地には乾燥に対する保護剤となるタンパク質や糖分が豊富にふくまれており、乾燥してもマイコプラズマが十分生きているという指摘が McGarity らによって既になされている。

こうした諸点に注意を払って培養実験を行うには研究者自らが、日常的にマイコプラズマ汚染は排除すべきであるという強い意識を持つことが有効であると思われる。今後、マイコプラズマ汚染に関する全国調査をさらに進めると共に、汚染していたマイコプラズマ種の同定も行い、汚染経路の特定なども試み注意を促したいと考えている。